

Oxygen vacancy trapping in tetragonal ZrO_2 studied by $^{111}\text{In}/\text{Cd}$ perturbed angular correlation

Niels Mommer, Theresa Lee, and John A. Gardner
Department of Physics, Oregon State University, Corvallis, Oregon 97331

William E. Evenson
Brigham Young University, Provo, Utah 84602
(Received 25 May 1999; revised manuscript received 21 July 1999)

Perturbed angular correlation (PAC) spectroscopy using dilute $^{111}\text{In}/\text{Cd}$ as the probe atom was used to measure the average electric field gradient (EFG) at Cd in high-temperature tetragonal zirconia, both nondoped and lightly doped with niobium or yttrium. The time-average EFG is reduced and strongly temperature dependent when oxygen vacancies are present—an effect attributed to a reduction of the average EFG when a vacancy is trapped at Cd. The doping and temperature dependence of the average EFG indicate that oxygen vacancies are trapped at first-neighbor positions to Cd with binding energy 0.62 (3) eV and at second neighbor positions to Y with binding energy 0.28 (5) eV. The average EFG when a vacancy is trapped by Cd is found to be zero. Samples were produced by precipitation from ZrOCl_2 solutions to which a few parts per 10^9 $^{111}\text{InCl}$ was added. Y- or Nb-doped samples had Y/Zr or Nb/Zr ratios up to 0.005. Calcining at 800 °C followed by a 1400 °C anneal produced good quality tetragonal phase powders with oxygen vacancy to oxygen ion ratios between 0 and 1500 ppm, depending on doping. The tetragonal phase could be supercooled for measurement to 1000 °C or lower.

I. INTRODUCTION

Perturbed angular correlation (PAC), in common with Mössbauer spectroscopy, nuclear magnetic resonance, and other techniques of nuclear solid-state physics, measures the electric and magnetic hyperfine interactions of probe nuclei in condensed matter. Thus the probe atom can be used to measure the characteristics of the electric field gradient (EFG) of the material in which it is immersed. For zirconia, $^{181}\text{Hf}/\text{Ta}$ PAC has been used to obtain information about phases,¹ lattice distortion,² or the mobility of oxygen vacancies.^{3,4} $^{111}\text{In}/\text{Cd}$ PAC is particularly well suited for use as a probe of oxygen vacancy properties because of the strong attractive electrostatic interaction between the Cd^{2+} probe ion and an oxygen vacancy. At high temperatures $^{111}\text{In}/\text{Cd}$ PAC frequencies are found to be strongly dependent on temperature and the concentration of oxygen vacancies.⁵⁻⁷ Such frequency dependence is unusual; no such dependence is observed with $^{181}\text{Hf}/\text{Ta}$ PAC.^{1,3} The unusual behavior occurs because the average EFG at the Cd probe ion is reduced when an oxygen vacancy is trapped, and vacancy motion is rapid enough that only the time-average frequency is observed. This time-average EFG and the observed quadrupole frequency become small when the oxygen vacancy trapping probability becomes large.

The analysis of PAC spectra is very complicated when modest local variations of the sample environment can mask the interactions of interest. Typical environmental effects include interactions with random dopants or impurities as well as strain and extended defects. Previous studies in our laboratory and others have been limited by inability to make reproducible samples of controlled vacancy concentrations and uniform distribution of oxygen vacancies. The present report includes results from PAC measurements of higher-quality samples as well as a reexamination of prior data

based on a better understanding of the interaction of Cd^{2+} with random lattice imperfections and Y^{3+} with oxygen vacancies.

II. EXPERIMENTAL DETAILS

A. Sample-making procedure

The samples were made by precipitation from high-purity or Y- or Nb-doped ZrOCl_2 solutions to which a few parts per 10^9 (ppb) of radioactive ^{111}In were added as InCl solution. ^{111}In has a half-life of 2.8 days, and it is possible to gather useful PAC data for only three or four half-lives before samples become too weak to be useful. Consequently, it is possible to make no more than a dozen or so PAC measurements before it is necessary to make a fresh sample.

The Y-doped solutions were prepared by adding a solution of yttrium nitrate, prepared by dissolving high-purity yttrium metal chips in excess nitric acid solution, to a zirconium oxychloride solution. Such solutions are clear and indefinitely stable. The niobium solutions were made by adding an oxalic acid solution of niobium hydroxide cake prepared by hydrolyzing niobium pentachloride, to a zirconium oxychloride solution. Such solutions are clear but may slowly develop a fine precipitate on the time scale of months. Only clear, water-white solutions are converted to PAC samples. These are prepared by addition of the metal-bearing solutions (concentration 20 g ZrOCl_2 per l) after mixing with a few drops of $^{111}\text{InCl}$ solution to a large excess of ammonium hydroxide, insuring thorough coprecipitation. After filtering, the resulting precipitate was then calcined at 800 °C and annealed at 1400 °C. Microstructure and crystallization kinetics of zirconia are known to depend on processing conditions.^{8,9} The annealing treatment prior to measurements resulted in fine white powders with grain sizes of

about 300 nm. Room-temperature x-ray diffraction measurements of well-annealed samples detected no other phases besides monoclinic zirconia.

Samples with negligible vacancy concentration can be made by doping with pentavalent Nb. Doping with trivalent Y creates oxygen vacancies to preserve electrical neutrality. Thus doping with 0.1 at% Y will create 250 ppm oxygen vacancies. Note that the Y concentration refers to total metal atoms in the sample, whereas oxygen vacancies are counted with respect to the number of oxygen atoms in the sample.

Using pure ZrOCl₂ solutions, i.e., neither doped by Y nor Nb, resulted in samples which were invariably doped by impurities, which we were unable to eliminate entirely. In the following paragraphs these unintentionally doped samples are, for brevity, called “nondoped.” The vacancy concentration of approximately 150 ppm in nondoped samples is presumably caused by transition metal and other impurity dopants present in our stock solutions and introduced during the sample-making process. This accidental doping by impurities is equivalent to approximately 600 ppm yttrium and is approximately the same in all samples.

All measured samples contain at least several hundred ppm of dopants or impurities, and the concentration of intrinsic oxygen vacancies is completely negligible.¹⁰ Therefore the concentration of oxygen vacancies can safely be assumed to be independent of temperature.

B. ¹¹¹In/Cd PAC in *t*-ZrO₂

¹¹¹In decays by electron capture to ¹¹¹Cd. The PAC measurements were carried out with the 171–245 keV $\gamma\gamma$ cascade of ¹¹¹Cd. In nonmagnetic materials, such as zirconia, PAC allows the measurement of the hyperfine interaction between the nuclear quadrupole moment Q of the $I=5/2$ intermediate state of the $\gamma\gamma$ cascade and the EFG at the probe site. The EFG causes a perturbation of the angular distribution of the radiation, γ_2 relative to γ_1 . This perturbation can be described by the “perturbation factor” $G_2(t)$. For a static interaction in polycrystalline samples, it is expressed as¹¹

$$G_2(t) = S_{20} + \sum_{n=1}^3 S_{2n} \cos(\omega_n t) \exp(-\delta \omega_n t), \quad (1)$$

where the transition frequencies ω_n between the sublevels of the intermediate nuclear state are functions of the quadrupole interaction frequency, $\omega_Q = eQV_{zz}/4I(2I-1)\hbar$, and the asymmetry parameter $\eta = (V_{xx} - V_{yy})/V_{zz}$, V_{ii} being the components of the diagonalized EFG tensor. For a Lorentzian line shape the broadening of the transition frequencies ω_n is described by δ , which represents the distribution width around the mean value of the EFG.

Frauenfelder and Steffen¹¹ give the dependence of the transition frequencies ω_n on ω_Q and η as

$$\begin{aligned} \omega_1 &= 2\sqrt{3}\alpha\omega_Q \sin\left[\frac{1}{3} \arccos \beta\right], \\ \omega_2 &= 2\sqrt{3}\alpha\omega_Q \sin\left[\frac{1}{3}(\pi - \arccos \beta)\right], \\ \omega_3 &= 2\sqrt{3}\alpha\omega_Q \sin\left[\frac{1}{3}(\pi + \arccos \beta)\right], \end{aligned} \quad (2)$$

with $\alpha = \sqrt{\frac{28}{3}(\eta^2 + 3)}$ and $\beta = \sqrt{80(1 - \eta^2)/\alpha^3}$.

If the EFG has precisely tetragonal symmetry, η equals 0 and $\omega_n = 6n\omega_Q$. Although the site symmetry in ZrO₂ is tetragonal, few sites actually have this symmetry, since structural defects and impurities give rise to a slight distortion of the tetragonal symmetry, causing η to be nonzero.

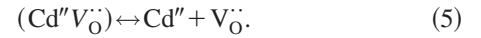
The half-life of the intermediate state of ¹¹¹Cd is about 85 ns.¹² At temperatures above about 1000 °C, movement of oxygen vacancies is so fast that the PAC frequencies are determined by the time-average EFG. For the case of an oxygen vacancy trapped by a Cd probe atom, the complex of probe atom and vacancy ($\text{Cd}''V_{\text{O}}^{\cdot\cdot}$) can have several orientations and only the averaged EFG over all orientations $\langle V_{zz \text{ vac}} \rangle$ is relevant for PAC. Also, since a vacancy traps and detraps many times during the lifetime of the intermediate state of the ¹¹¹Cd probe atom, only a time-weighted average of $\langle V_{zz \text{ vac}} \rangle$ and $V_{zz \text{ lat}}$, the EFG of a vacancy-free lattice, is observed. If f is the fraction of time a vacancy is trapped by a Cd ion, the observed EFG can be written as

$$\langle V_{zz} \rangle = (1-f)V_{zz \text{ lat}} + f\langle V_{zz \text{ vac}} \rangle, \quad (3)$$

or, more conveniently, the observed quadrupole frequency $\langle \omega_Q \rangle$ is

$$\langle \omega_Q \rangle = (1-f)\omega_{Q \text{ lat}} + f\langle \omega_{Q \text{ vac}} \rangle. \quad (4)$$

Oxygen vacancies are effectively doubly positively charged and therefore attracted by the divalent Cd probe atoms, which are effectively doubly negatively charged. This results in the formation of ($\text{Cd}''V_{\text{O}}^{\cdot\cdot}$) complexes with a binding energy Q_{Cd} . The concentration of free vacancies is controlled by the dissociation of the ($\text{Cd}''V_{\text{O}}^{\cdot\cdot}$) complex, i.e.,



The number of orientations, N_{Cd} of these ($\text{Cd}''V_{\text{O}}^{\cdot\cdot}$) complexes (i.e., $N=8$ for a nearest-neighbor position of the oxygen vacancy and $N=24$ for a second neighbor) and their binding energy Q_{Cd} determine then the concentrations of these complexes [$\text{Cd}''V_{\text{O}}^{\cdot\cdot}$], free Cd atoms [Cd''] and free oxygen vacancies [$V_{\text{O}}^{\cdot\cdot}$] by a mass-action equation¹³

$$[\text{Cd}''][V_{\text{O}}^{\cdot\cdot}]/[\text{Cd}''V_{\text{O}}^{\cdot\cdot}] = N_{\text{Cd}}^{-1} \exp(-Q_{\text{Cd}}/kT). \quad (6)$$

We can then write the fraction f of Cd atoms which have a vacancy trapped as

$$\begin{aligned} f &= [\text{Cd}''V_{\text{O}}^{\cdot\cdot}]/([\text{Cd}''V_{\text{O}}^{\cdot\cdot}] + [\text{Cd}'']) \\ &= \left[\frac{1}{N_{\text{Cd}}c} \exp(-Q_{\text{Cd}}/kT) + 1 \right]^{-1}, \end{aligned} \quad (7)$$

where $c = [V_{\text{O}}^{\cdot\cdot}]$ is the concentration of free oxygen vacancies. We emphasize that c is the free vacancy concentration, not the total vacancy concentration. While Cd is present only at the ppb level and the effect of ($\text{Cd}''V_{\text{O}}^{\cdot\cdot}$) complexes on the free vacancy concentration can therefore be neglected, the effect of dopants, e.g., ($\text{Y}'V_{\text{O}}^{\cdot\cdot}$) complexes, has to be considered for Y-doped samples. Kilner *et al.*¹⁴ have shown that bound complexes can significantly affect the population of

free vacancies, especially at lower temperatures. For samples with an yttrium concentration c_Y , a fraction f_Y of all vacancies is trapped at any time by Y ions, and the total vacancy concentration c_{tot} is given by

$$c_{\text{tot}} = \frac{c}{1-f_Y} = c \left[1 + \frac{1}{2} N_Y c_Y \exp(Q_Y/kT) \right], \quad (8)$$

where N_Y and Q_Y denote the number of orientations and binding enthalpy of a $(Y'V_{\text{O}})$ complex, respectively. The factor of $\frac{1}{2}$ arises from counting Y atoms with respect to metal atoms, whereas oxygen vacancies are counted with respect to oxygen atoms.

Combining Eqs. (4), (7), and (8) permits the measured quadrupole interaction frequency to be expressed as

$$\langle \omega_Q \rangle = \omega_{Q \text{ Lat}} - \frac{\omega_{Q \text{ lat}} - \langle \omega_{Q \text{ vac}} \rangle}{(1/N_{\text{Cd}} c_{\text{tot}}) [1 + \frac{1}{2} N_Y c_Y \exp(Q_Y/kT)] \exp(-Q_{\text{cd}}/kT) + 1}. \quad (9)$$

With Eq. (9), the binding enthalpies Q_{Cd} and Q_Y , as well as the number of orientations of the $(\text{Cd}''V_{\text{O}})$ and $(Y'V_{\text{O}})$ complexes, can be determined from PAC spectra taken over a temperature range from samples with controlled vacancy concentrations. Provided that the fraction of time a Cd probe atom has a vacancy trapped is the same as in thermal equilibrium, Eq. (9) is correct. Strictly speaking, however, this is only an approximation since $^{111}\text{Cd}^{2+}$ probe ions are created by decay of $^{111}\text{In}^{3+}$ ions, and it therefore takes a finite time for the concentration of “free” probe atoms to come into thermal equilibrium with the $(\text{Cd}''V_{\text{O}})$ complexes, as implied by Eqs. (4) and (5). The jump rate of oxygen atoms, τ , can be estimated from the Debye frequency ν_D and the activation enthalpy for hopping, $Q=0.5 \text{ eV}$, to be about $\tau \approx \nu_D \exp(-Q/kT)$, which should be several orders of magnitude smaller than the lifetime of the intermediate state of ^{111}Cd (85 ns) for temperatures above 1000 °C. Hence it can be safely assumed that the PAC spectra give information about the equilibrium fraction of Cd probe ions forming $(\text{Cd}''V_{\text{O}})$ complexes. In order to analyze spectra taken at lower temperatures, we have developed more sophisticated stochastic models that include in one model the effects of a trapped vacancy hopping around the Cd probe ion as well as trapping and detrapping.¹⁵ At high temperatures, where the jump rates τ are fast, as described in this paragraph, the stochastic models give the same temperature dependence for the time-average EFG as discussed in this paper.

Random static defects cause a distribution of η and V_{zz} . Therefore the average of η will be nonzero. Hence a static broadening of the observed transition frequencies ω_1 , ω_2 , and ω_3 will occur. This broadening of the transition frequencies leads also to a broadening of the quadrupole interaction frequency ω_Q , but not to a change of the average of ω_Q , at least as long as η is small.^{16,17}

III. EXPERIMENTAL RESULTS

Figure 1 shows PAC spectra of a Nb-doped sample and a 0.1 at.% Y-doped sample together with their Fourier transforms. While samples doped with pentavalent Nb contain only a negligible amount of vacancies, the Y-doped sample contains about 400 ppm oxygen vacancies, 250 ppm to charge compensate for the Y and about 150 ppm due to the unavoidable impurities mentioned above. The Y-doped sample clearly shows a lower quadrupole interaction fre-

quency ω_Q than the Nb-doped sample.

Figure 2 shows that lowering the temperature greatly lowers the quadrupole interaction frequency for samples containing oxygen vacancies (nondoped and Y doped), whereas ω_Q shows a slight increase for the vacancy-free Nb-doped sample. For a given temperature it is also evident that the higher the vacancy concentration, or Y-doping level, the lower the quadrupole interaction frequency.

A few tenths of a percent of Nb doping is sufficient to compensate all the oxygen vacancies associated with the unavoidable impurities mentioned above. In such sufficiently Nb-doped samples, the observed quadrupole interaction frequency is the quadrupole interaction frequency of the vacancy-free lattice $\omega_{Q \text{ lat}}$, which shows a small dependence on temperature. Such small EFG temperature dependences are common and attributable to such things as thermal expansion, atomic vibrational amplitude changes with T , etc.¹⁸ A linear fit to the temperature dependence of ω_Q gives

$$\omega_{Q \text{ lat}}(T) = 6.75(1) \text{ Mrad/s} - 4.12(7) \times 10^{-4} \text{ Mrad/(s K)} \times T. \quad (10)$$

Attributing the lower quadrupole interaction frequencies of nondoped and Y-doped samples to the effect of $(\text{Cd}''V_{\text{O}})$ complexes, as discussed in Sec. II B above, the temperature dependence of the observed quadrupole interaction frequencies could be fitted to Eq. (9) using Eq. (10). A numerical analysis yielded $Q_{\text{Cd}}=0.62(3) \text{ eV}$ for the binding enthalpy of an oxygen vacancy to a Cd ion and $N_{\text{Cd}}=7.8(3)$ for the number of possible orientations of the $(\text{Cd}''V_{\text{O}})$. The number of equivalent sites at which a vacancy can be trapped by a Cd ion is therefore approximately equal to the number of first-neighbor trap positions. For the binding enthalpy of a vacancy to an Y ion, the fit gave $Q_Y=0.28(5) \text{ eV}$ with $N_Y=23.2(10)$, so that the number of sites for a vacancy trapped by an Y ion is, within experimental uncertainty, equal to 24, the number of second-neighbor trap sites. The fitting results also gave the average EFG over all possible orientations of a Cd-ion–vacancy pair $(\text{Cd}''V_{\text{O}})$ as $\langle \omega_{Q \text{ vac}} \rangle = 0(1) \text{ Mrad/s}$.

For Nb-doped samples an increase in Nb concentration from several hundred ppm to 5000 ppm caused the asymmetry parameter η to increase from about 0.06 up to 0.22. As mentioned in the previous section, an increasing η is accompanied by an increased linewidth of the transition frequen-

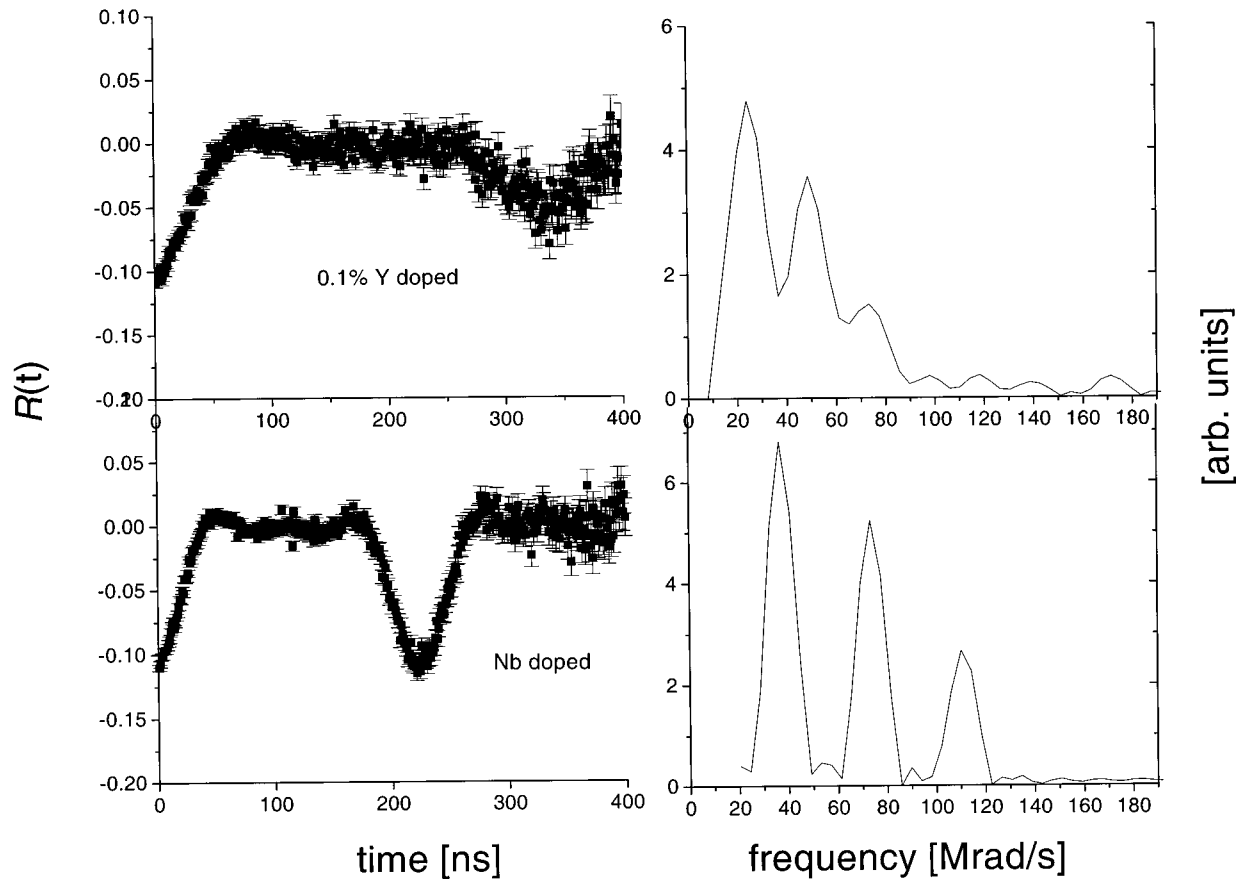


FIG. 1. PAC spectra of Nb- and Y-doped tetragonal zirconia samples at 1200 °C and their Fourier transforms.

cies ω_n . The spectra of various Nb-doped samples, which were effectively free of oxygen vacancies, were fitted to Lorentzian line shapes. As can be seen in Fig. 3, an increase of η correlates with an increase in the spectral linewidth of the transition frequencies. The observed quadrupole interaction frequencies are independent of linewidth. For the non-

doped samples η is below 0.06 and for 0.1- at. % Y-doped samples below 0.16. With increasing Y content the asymmetry parameter η increased up to $\eta=0.21$ for 0.5- at. % Y-doped samples at 1400 °C. In general, η increased with decreasing temperature, an effect which was most pronounced for highly Y-doped samples.

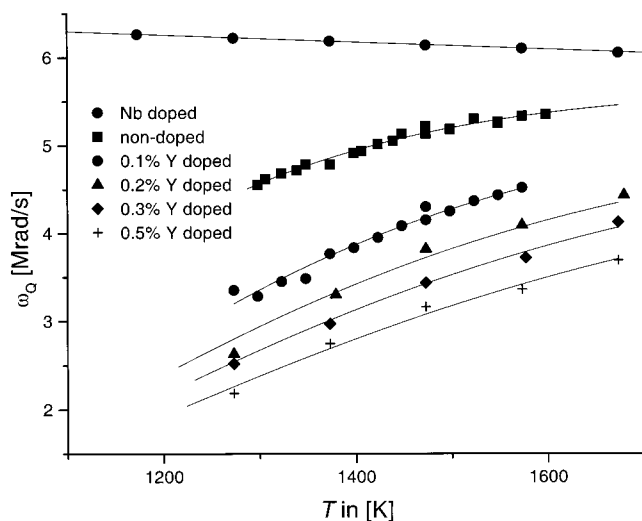


FIG. 2. Quadrupole interaction frequencies ω_Q for a Nb-doped, nondoped, and Y-doped sample with 0, 180, 440, 760, 1020, and 1430 ppm oxygen vacancies, respectively. The solid lines show fits to Eq. (9).

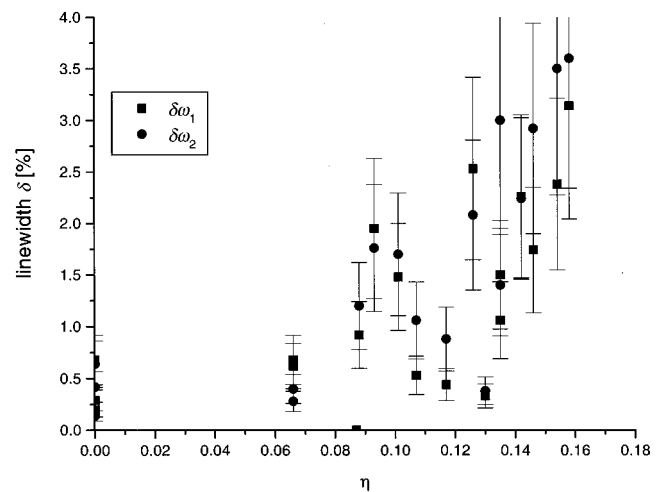


FIG. 3. Linewidth δ of the transition frequencies ω_1 and ω_2 , resulting from fits to a Lorentzian line shape, for various Nb-doped samples plotted vs the asymmetry parameter η . The increase of δ with η does not affect the value of ω_Q , which is independent of η .

IV. DISCUSSION

A. Defect properties

PAC measurements of tetragonal zirconia samples with oxygen vacancy concentrations ranging from 0 to 1400 ppm show a clear reduction of the quadrupole interaction frequency ω_Q with decreasing temperature and increasing vacancy concentration. This reduction of ω_Q is attributed to the trapping of oxygen vacancies by Cd probe ions. During a fraction f of the lifetime of the intermediate state, a Cd probe atom has an oxygen vacancy trapped. As a result of the fast motion of oxygen atoms, the measured quadrupole interaction frequency corresponds to the average EFG for the various sites among which the vacancy jumps, as given by Eq. (4). Numerical analysis of the PAC spectra shows that the EFG averaged over the orientations of a $(\text{Cd}''\text{V}_\text{O}'')$ complex is zero within experimental accuracy. This indicates that significant lattice relaxation takes place around a vacancy. One scenario consistent with this observation is that the lattice is cubic in a substantial volume around an oxygen vacancy. Although not the only explanation for our observation, it is a tempting speculation because it gives a very simple picture of why large vacancy densities, whether introduced by cation or anion doping¹⁹ or depletion of oxygen,¹⁰ are accompanied by a stabilization of the high-temperature cubic phase.

The present PAC results show clearly that an oxygen vacancy is trapped by a Cd^{2+} ion in a nearest-neighbor site ($N_{\text{Cd}}=8$) with a binding enthalpy of $Q_{\text{Cd}}=0.62(3)$ eV. An earlier analysis of PAC studies^{5,7} was erroneous (giving N_{Cd} closer to 24 than 8 and Q_{Cd} approximately 0.44 eV). The major error in these previous analyses arose from an oversimplified correction for effects of static broadening, as discussed below. The present analysis also includes a correction for effects of trapping of oxygen vacancies by Y^{3+} ions in Y-doped samples and gives additional quantitative results about $(\text{Y}'\text{V}_\text{O}'')$ complexes. These complexes are found to have a binding enthalpy of $Q_{\text{Y}}=0.28(5)$ eV with the oxygen vacancy being in a next-nearest-neighbor site ($N_{\text{Y}}=24$). We are aware of no other data on the binding enthalpy of $(\text{Y}'\text{V}_\text{O}'')$ complexes in tetragonal zirconia, but for cubic zirconia Manning *et al.* found $Q_{\text{Y}}=0.26$ eV (Ref. 13) using tracer diffusion measurements. The unit cell dimensions of tetragonal and cubic zirconia are almost the same and, particularly in view of the lattice relaxation, one might expect the binding enthalpies to be similar in the two phases, consistent with our results.

The numerical results of $N_{\text{Cd}}=8$ and $N_{\text{Y}}=24$ imply that Cd^{2+} , which is smaller than Zr^{4+} , traps oxygen vacancies at a nearest-neighbor position, whereas Y^{3+} , which is larger than Zr^{4+} , traps vacancies in a next-nearest-neighbor position. An x-ray absorption study by Li *et al.* also found that oxygen vacancies in tetragonal zirconia prefer a next-nearest-neighbor site relative to yttrium.²⁰ Both of our results on $(\text{Y}'\text{V}_\text{O}'')$ and $(\text{Cd}''\text{V}_\text{O}'')$ complexes are also in agreement with expectations based on both experimental^{20,21} and theoretical evidence,²² that smaller cations generally favor a nearest-neighbor site, while larger ones tend to favor a next-nearest-neighbor site.

The present results complement $^{181}\text{Hf}/\text{Ta}$ PAC results where oxygen vacancies are not attracted by the probe atom and their movement leads to a damping of the PAC signal.

Rivas *et al.*³ used $^{181}\text{Hf}/\text{Ta}$ PAC to determine the activation enthalpy of the PAC damping to be $Q_m=0.50(4)$ eV in Y-doped tetragonal zirconia (Y-TZP). Gardner *et al.*⁴ had earlier used $^{181}\text{Hf}/\text{Ta}$ PAC to find the activation enthalpy of PAC damping in Y-doped cubic zirconia to be 1.0(1) eV. Both authors identify this activation enthalpy as the activation enthalpy of oxygen vacancy motion (hopping). The large difference is surprising, since one might expect oxygen vacancy hopping to have similar activation enthalpies in these to similar lattices. Neither is directly related to the present study, however, which gives no direct information on vacancy hopping enthalpy. However, further $^{111}\text{In}/\text{Cd}$ PAC work that includes careful line shape analysis with stochastic models¹⁵ should eventually provide information on vacancy hopping.

B. Static broadening analysis

Static broadening of $^{111}\text{In}/\text{Cd}$ PAC frequencies is small for nondoped and very lightly doped samples. The magnitude of the line broadening is larger for a given impurity density than what was observed by $^{181}\text{Hf}/\text{Ta}$ PAC.⁴ This sensitivity may indicate that the local environment of Cd is more easily polarized by small lattice distortions than that of Ta and enhances the effects of line broadening.

The large line broadening causes the symmetry at different sites to be less than axial so that the average η is greater than zero. However, the average ω_Q is unaffected by line broadening. Consequently, the model developed in Sec. II B, which ignores line broadening, is valid for fitting the experimental ω_Q results. In prior analyses,^{5,7} ω_Q was taken as proportional to ω_1 and therefore not properly corrected for the effect of line broadening.

One apparent peculiarity noted in Sec. III is that η and line broadening become larger for doped samples as temperature is reduced. This is a result of the decrease of ω_Q with temperature, not any significant change in the EFG contributions due to impurities and other defects. The ratio of the static EFG broadening to the average ω_Q increases with decreasing temperature because the denominator decreases. The experimental line broadening is proportional to this ratio, and the η shift is a monotonically increasing function of this ratio. Hence both increase as temperature decreases.

V. SUMMARY AND CONCLUSION

The trapping of oxygen vacancies by Cd^{2+} and Y^{3+} ions in tetragonal zirconia was investigated by $^{111}\text{In}/\text{Cd}$ PAC. Zirconia samples with oxygen vacancy levels ranging from 0 to 1500 ppm were produced by doping with either Nb or Y. PAC spectra of these samples show a decreasing quadrupole interaction frequency ω_Q both with decreasing temperature and increasing vacancy concentration. This decrease in ω_Q is attributed to the formation of $(\text{Cd}''\text{V}_\text{O}'')$ complexes, that is, the trapping of oxygen vacancies by ^{111}Cd probe atoms. The trapping and detrapping of vacancies occurs on a time scale which is at least two orders of magnitude faster than the lifetime of the intermediate state of the ^{111}Cd probe atom. As a result, only an average EFG(ω_Q) for the possible configurations of Cd probe atoms, i.e., with and without a trapped vacancy, is observed. This observed average gives the frac-

tion of Cd probe atoms which have a vacancy trapped. Using a simple model, the observed quadrupole interaction frequency ω_Q can therefore be written as a function of the concentration of free oxygen vacancies, the binding enthalpy Q_{Cd} of a vacancy to a Cd ion and temperature. Owing to the trapping of oxygen vacancies by Y, the free vacancy concentration is in turn a function of the total vacancy concentration (Y content), the binding enthalpy Q_Y of a vacancy to an Y ion, and temperature. Using a numerical analysis of the temperature dependence of ω_Q for samples with various doping levels, it was found that a Cd²⁺ ion traps an oxygen vacancy

in a nearest-neighbor position with a binding enthalpy of $Q_{Cd}=0.62(3)$ eV and that an Y³⁺ ion traps an oxygen vacancy in a next-nearest-neighbor position with a binding enthalpy of $Q_Y=0.28(5)$ eV.

ACKNOWLEDGMENTS

The authors thank Dr. J. A. Sommers at Oremet-Wah Chang, Albany, for providing the ZrOCl₂ solutions. The financial support of the Alexander von Humboldt Foundation for N. Mommer is gratefully acknowledged.

-
- ¹H. Jaeger, J. A. Gardner, J. C. Haygarth, and R. L. Rasera, *J. Am. Ceram. Soc.* **69**, 458 (1986).
- ²M. Forker, U. Brossmann, and R. Würschum, *Phys. Rev. B* **57**, 5177 (1998).
- ³P. C. Rivas, M. C. Caracoche, A. F. Pasquevich, J. A. Martínez, A. M. Rodríguez, A. R. López García, and S. R. Mintzer, *J. Am. Ceram. Soc.* **79**, 831 (1996).
- ⁴J. A. Gardner, H. Jaeger, H. T. Su, W. H. Warnes, and J. C. Haygarth, *Physica B* **150**, 223 (1988).
- ⁵H.-T. Su, R. Wang, H. Fuchs, J. A. Gardner, W. E. Evenson, and J. A. Sommers, *J. Am. Ceram. Soc.* **73**, 3215 (1990).
- ⁶R. Wang, J. A. Gardner, W. E. Evenson, and J. A. Sommers, *Phys. Rev. B* **47**, 638 (1993).
- ⁷R. Platzer, E. Karapetrova, M. O. Zacate, J. A. Gardner, J. A. Sommers, and W. E. Evenson, *Mater. Sci. Forum* **239-241**, 57 (1997).
- ⁸R. P. Denkwicz, K. S. TenHuisen, and J. Adair, *J. Mater. Res.* **5**, 2698 (1990).
- ⁹B. H. Davis, *J. Am. Ceram. Soc.* **67**, c-168 (1984).
- ¹⁰W. Wang and D. R. Olander, *J. Am. Ceram. Soc.* **76**, 1242 (1993).
- ¹¹H. Frauenfelder and R. M. Steffen, in *Alpha-, Beta- and Gamma-Ray Spectroscopy*, edited by K. Siegbahn (North-Holland, Amsterdam, 1965), Vol. 2, Chap. XIX, pp. 997–998.
- ¹²B. Harmatz, *Nucl. Data Sheets* **27**, 453 (1979).
- ¹³P. S. Manning, J. D. Sirman, R. A. De Souza, and J. A. Kilner, *Solid State Ionics* **100**, 1 (1997).
- ¹⁴J. A. Kilner and C. D. Waters, *Solid State Ionics* **6**, 253 (1982).
- ¹⁵W. E. Evenson, Jun Lu, M. W. Winz, J. A. Gardner, M. O. Zacate, T. Lee, and N. Mommer, *Hyperfine Interact.* **120/121**, 427 (1999).
- ¹⁶M. Forker, *Nucl. Instrum. Methods* **106**, 121 (1973).
- ¹⁷M. Forker, W. Herz, and D. Simon, *Nucl. Instrum. Methods Phys. Res. A* **337**, 534 (1994).
- ¹⁸J. Christiansen, P. Heubes, R. Keitel, W. Klinger, W. Loeffler, W. Sandner, and W. Witthuhn, *Z. Phys. B* **24**, 177 (1976).
- ¹⁹M. Lerch and O. Rahäuser, *J. Mater. Sci.* **32**, 1357 (1997).
- ²⁰P. Li, I.-W. Chen, and J. E. Penner-Hahn, *J. Am. Ceram. Soc.* **77**, 118 (1994).
- ²¹C. R. A. Catlow, A. V. Chadwick, G. N. Greaves, and L. M. Moroney, *J. Am. Ceram. Soc.* **69**, 272 (1986).
- ²²L. Minervini, M. O. Zacate, and R. W. Grimes, *Solid State Ionics* **116**, 339 (1999).